HHS Public Access

Author manuscript

J Control Release. Author manuscript; available in PMC 2024 March 01.

Published in final edited form as:

J Control Release. 2023 March ; 355: 149–159. doi:10.1016/j.jconrel.2023.01.065.

SEX-BASED DIFFERENCES OF ANTIOXIDANT ENZYME NANOPARTICLE EFFECTS FOLLOWING TRAUMATIC BRAIN INJURY

Aria W. Tarudji[a], **Hunter A. Miller**[a,b], **Evan T. Curtis**[a], **Christopher L. Porter**[b], **Gary L. Madsen**[b], **Forrest M. Kievit**[a,*]

[a]Department of Biological Systems Engineering, University of Nebraska – Lincoln, 262 Morrison Center, Lincoln, NE, 68583, USA

[b]ProTransit Nanotherapy, 16514L St., Omaha, NE, 68135, USA

Abstract

Following traumatic brain injury (TBI), reactive oxygen species (ROS) are released in excess, causing oxidative stress, carbonyl stress, and cell death, which induce the additional release of ROS. The limited accumulation and retention of small molecule antioxidants commonly used in clinical trials likely limit the target engagement and therapeutic effect in reducing secondary injury. Small molecule drugs also need to be administered every several hours to maintain bioavailability in the brain. Therefore, there is a need for a burst and sustained release system with high accumulation and retention in the injured brain. Here, we utilized Pro-NP™ with a size of 200 nm, which was designed to have a burst and sustained release of encapsulated antioxidants, Cu/Zn superoxide dismutase (SOD1) and catalase (CAT), to scavenge ROS for more than 24 h post-injection. Here, we utilized a controlled cortical impact (CCI) mouse model of TBI and found the accumulation of Pro-NP™ in the brain lesion was highest when injected immediately after injury, with a reduction in the accumulation with delayed administration of 1 h or more post-injury. Pro-NP™ treatment with 9,000 U/kg SOD1 and 9,800 U/kg CAT gave the highest reduction in ROS in both male and female mice. We found that Pro-NP™ treatment was effective in reducing carbonyl stress and necrosis at 1 d post-injury in the contralateral hemisphere in male

*Correspondence: fkievit2@unl.edu; Tel.: +1-402-472-2175.

AUTHOR CONTRIBUTIONS

G.M., A.T., and F.K. conceived and designed the study. G.M. and C.P. synthesized and characterized the NPs. A.T., H.M., and E.C. performed the in vivo experiments. All authors analyzed the data and participated in the discussion, figure preparation, and writing of the manuscript.

DECLARATION OF INTEREST

The study was in collaboration with ProTransit Nanotherapy, LLC, Omaha, NE, a start-up company based on patented work done at the University of Nebraska Medical Center. G.M. is founder of ProTransit Nanotherapy and has an equity interest in the company. ProTransit can make Pro-NP™ available to potential investigators under material transfer agreement.

Credit author statement

G.M., A.T., and F.K. conceived and designed the study. G.M. and C.P. synthesized and characterized the NPs. A.T., H.M., and E.C. performed the in vivo experiments. All authors analyzed the data and participated in the discussion, figure preparation, and writing of the manuscript.

mice, which showed a similar trend to untreated female mice. Although we found that male and female mice similarly benefit from Pro-NP™ treatment in reducing ROS levels 4 h post-injury, Pro-NP™ treatment did not significantly affect markers of post-traumatic oxidative stress in female CCI mice as compared to male CCI mice. These findings of protection by Pro-NP™ in male mice did not extend to 7 d post-injury, which suggests subsequent treatments with Pro-NP™ may be needed to afford protection into the chronic phase of injury. Overall, these different treatment effects of Pro-NP™ between male and female mice suggest important sex-based differences in response to antioxidant nanoparticle delivery and that there may exist a maximal benefit from local antioxidant activity in injured brain.

Graphical Abstract

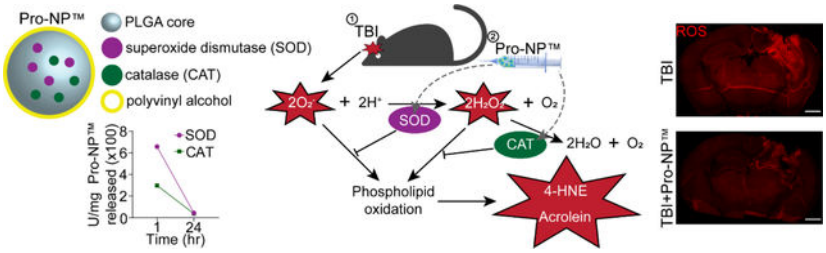

Keywords

traumatic brain injury; reactive oxygen species; lipid peroxidation products; treatment window; PLGA nanoparticles; carbonyl stress

1. Introduction

Traumatic brain injury (TBI) can be caused by either a penetrating or non-penetrating blow to the head that results in compression, deformation, displacement, stretching, shearing, tearing, and crushing of the brain and blood vessels [1]. This primary injury is then followed by a cascade of biochemical derangements that range from the release of calcium, excitatory amino acids, and oxidative stress to carbonyl stress, mitochondrial dysfunction, neuroinflammation, and cell death. This secondary injury can last years to decades post-injury [2–4] and spread to the contralateral hemisphere [5, 6].

Reactive oxygen species (ROS), such as superoxides, are produced in the electron transport chain in the mitochondria. Under physiological conditions, ROS production is countered by superoxide dismutase (SOD) and catalase (CAT), producing water and oxygen. However, following TBI, ROS are produced at elevated rates while endogenous antioxidant enzymes are produced at lower rates [7–9]. Excess ROS oxidize DNA, proteins, and lipids, resulting in DNA damage, lipid peroxidation products (LPOx), neuroinflammation, and neurodegeneration. Therefore, antioxidant therapies, such as PEG-conjugated SOD1 and PEG-conjugated CAT have been employed to improve outcomes following TBI in preclinical studies and phase I and II trials [10–13]. However, no TBI drug treatments have shown efficacy in phase III trials. The failure in TBI clinical trials might be caused by poor target engagement of therapeutic agents because of poor accumulation and retention

in the brain. The small molecule drugs also need to be administered every several hours to maintain the bioavailability within the therapeutic window [14–18]. Therefore, a new TBI treatment with high accumulation, retention, and prolonged release of therapy is needed.

The properties of nanoparticles (NPs) are highly adjustable, which can be exploited to provoke a desired response, such as higher accumulation and drug delivery into the brain. The controllable size of NPs is also ideal in TBI applications since the blood-brain barrier (BBB) is disrupted to various degrees following TBI, allowing enhanced permeability and retention of NPs in the injured brain [9, 19–25]. Higher accumulation and retention of NPs in brain injury are expected to increase the target engagement compared to the small molecule drugs, which may improve the therapeutic efficacy in reducing the progression of secondary injury. ROS scavenger NPs have also been shown to reduce secondary TBI markers [6, 26–35]. Therefore, antioxidant NPs have shown promising results for TBI treatment.

SOD and CAT are two of the endogenous antioxidant enzymes. Three of the most well known subtypes of SOD are SOD1 (copper/zinc-based cytosolic SOD), SOD2 (manganese based mitochondrial SOD), and SOD3 (copper/zinc-based extracellular SOD). Although the combination of SOD1 and CAT is promising for scavenging ROS, SOD and CAT are rapidly cleared from the blood circulation due to renal and hepatic clearance, respectively [36, 37]. Therefore, SOD1 and CAT have also been encapsulated in PLGA-based NPs to be slowly released over a period of 1 week, while keeping the encapsulated enzymes active and stable, as shown by the patent of Pro-NP™ [38], which increases the target engagement and prolongs delivery in the tissue of interest. Slowly releasing the antioxidant enzymes also enables distribution of the antioxidant enzymes in the cytosol and mitochondria [39], where the ROS are produced, compared to other antioxidant enzymes nanocarriers that might not escape from the nanocarriers in the endosome [40–43]. Another advantage of employing PLGA-based NPs are the low toxicity and high biodegradability of PLGA [44], FDA approval for drug delivery, as well as biocompatibility of PLGA NPs with antioxidant enzymes in protecting the neuron *in vitro* and *in vivo* [45–49]. Here, we utilized Pro-NP™, an SOD1 and CAT encapsulated PLGA-based NP that shows burst released within an hour of injection and sustained release for more than 24 h post-injection [38]. Combining sustained ROS scavenging activities with the accumulation and retention of Pro-NP™ following brain injury, we aimed to determine the effects of Pro-NP™ treatment on the progression of secondary injury following TBI.

One of the limitations of current TBI studies is that the majority of TBI research is carried out in male rodents or human subjects. However, sex plays a significant role in the outcome of TBI. For example, the outcomes of female TBI patients are often times worse in mild TBI, but better in severe TBI, as compared to the outcomes of male TBI patients [50, 51]. A similar trend is also found in rodent studies [51]. Thus, estrogen and progesterone were hypothesized to play a role in improving the outcomes of TBI although subsequent clinical trials did not establish significant improvement following TBI [52]. Recent studies also found that mitochondria in females are less prone to disruption from stress [53, 54] and employed different metabolism pathways [55]. Glial cells in females are also less activated in the subacute phase of injury [56, 57]. However, the exact correlation between

sex and the outcomes of TBI has not been fully understood. The behavior of nanomaterials, especially in TBI, also depend on the sex of the animal, in which female mice tend to have a higher accumulation of macromolecules and NPs with delayed injection [58]. Our previous study [6] also found that antioxidant nanoparticle therapy reduced the inflammation in the contralateral hemisphere in females at one month post-TBI, but only males benefit from the antioxidant treatment to improve spatial learning and memory following an injury. Therefore, there is a need to study the effect of sex on antioxidant enzymes loaded nanoparticles in reducing the secondary injury of TBI. The finding of this study may help to understand the success or failure of antioxidant therapies for TBI and stroke in clinical trials.

In this study, we utilized a severe controlled cortical impact (CCI) mouse model of TBI to the left cortex of male and female mice. Although CCI is not the most common cause of TBI in humans, CCI produces a similar secondary injury cascade to the secondary injury in humans [59, 60]. Moreover, CCI is highly reproducible and comparable between studies. We assessed the treatment window, therapeutic window, and optimum SOD1:CAT ratio of Pro-NP™ following brain injury, as well as the time-course of carbonyl stress and cell death in the acute and subacute phases of injury (1, 3, and 7 days post-TBI).

2. Methods and Materials:

2.1. Pro-NP™ synthesis

Pro-NP™ is a patented composition of poly(lactic-co-glycolic acid) (PLGA)-based biodegradable polymer NPs with superoxide dismutase (SOD1) and catalase (CAT) [38]. SOD1- and CAT-Pro-NP™ were synthesized and characterized separately to allow various SOD1:CAT ratios.

Gd-Pro-NP™ was synthesized as previously described [23]. Briefly, 85 mg of PLGA, 9 mg of (+)-dimethyl L-tartrate, 30 mg of human serum albumin (HSA), and 8.1 mg of 1, 2-distearoyl-sn-glycero-3-phosphoethanolamine-poly(ethylene glycol)-Gd was dissolved in dichloromethane (DCM). The DCM solution was then added into 3% w/v polyvinyl alcohol and sonicated for 3 min. After the DCM had evaporated, the Gd-Pro-NP™ was then washed three times via centrifugation with distilled water. The final pellet was resuspended in glucose solution and freeze dried. The dried powder was kept at −80 °C until further use.

Pro-NP™ and Gd-Pro-NP™ were redissolved in Dulbecco’s phosphate buffered saline (DPBS, Thermo Fisher Scientific, Waltham, MA) at desired concentrations (described below) before being injected intravenously in mice.

2.2. Pro-NP™ characterizations

The hydrodynamic diameter and zeta potential of Pro-NP™ were measured with dynamic light scattering. For assessing the serum stability of Pro-NP™, Pro-NP™ were resuspended in 0, 5, and 25% of fetal bovine serum in DPBS, and the hydrodynamic diameter of Pro-NP™ were measured with dynamic light scattering at 0, 1, 6, 24, and 48 h incubation at 37 °C.

The enzymatic activities of Pro-NP™ were measured with colorimetric SOD1 (S31110, Dojindo Molecular Technologies, Inc., Rockville, MD) and CAT (CAT100, Sigma-Aldrich, St. Louis, MO) activity assays collected at 1 and 24 h post-incubation of Pro-NP™ in PBS buffer (150 mM, pH 7.4) containing 0.1% w/v HSA at 37 °C following previously published procedures [48]. Gd content was measured with inductively coupled plasma mass-spectroscopy.

The blood elimination half-life of Pro-NP™ *in vivo* was estimated using artirial input function from the R1 mapping taken by MRI.

2.3. Controlled Cortical Impact Mouse Model of TBI

All animal procedures were performed in accordance with the approval of the University of Nebraska–Lincoln IACUC. The controlled cortical impact (CCI) mouse model of TBI was performed as described previously with some modifications [35]. Briefly, 8- to 10-week-old male and female C57BL/6J mice (Jackson Laboratory, Bar Harbor, ME, USA) were acclimated for at least three days. The average weight of 8-week-old male mice was 24.1 g and the average weight of 8-week-old female mice was 18.1 g. Mice were induced with isoflurane gas via inhalation. The hair of the scalp was removed, and the scalp was disinfected with betadine and isopropanol wipes. Lidocaine and bupivacaine were applied to the scalp, and buprenorphine SR was given subcutaneously. A midline incision was made on the scalp and a 2.5-mm trephine drill was used on the skull over the left frontoparietal cortex (2 mm anterior and 2 mm left of lambda), while keeping the dura intact. A 2-mm convex tip impacted normal to the dura surface to a depth of 2.5 mm, with a velocity of 4 m/s and a dwell time of 80 ms. The incision was closed using tissue adhesive. Experimentalists were not blinded throughout the study, but mice were assigned to treatment groups prior to surgeries.

Estrous was not controlled for in female mice at the time of injury because previous studies found that the estrous cycle stages at the time of the injury have little impact on neuroprotection in female rodents [61, 62]. Furthermore, controlled and random stages of the estrous cycle at the time of injury showed similar variability to male mice [56, 61–64].

2.4. *In vivo* Dynamic Contrast-Enhanced Magnetic Resonance Imaging (DCE-MRI)

In vivo NP assessment consisted of dynamic contrast-enhanced (DCE)-MRI using a 9.4T MRI system (Varian) equipped with a 4-cm Millipede RF imaging probe with triple-axis gradients (100 G/cm max). DCE-MRI was performed to compare the Gd-Pro-NP™ accumulation at various time-points following a CCI [21, 23, 35]. Briefly, mice were induced with isoflurane gas and maintained at 50 to 80 breaths per minute. Pre- and post-contrast R1 mapping were performed using the variable flip angle method with two angles, 10° and 30° [65, 66]. Mice were injected with a bolus administration of 100 μL of Gd-Pro-NP™ with 0.067 mM Gd concentration via tail vein catheter followed by 100 μL PBS to flush all remaining NP solution at various time points following the CCI. A series of T1-weighted gradient echo scans with a flip angle of 30°, repetition time (TR) of 54 ms, echo time (TE) of 2.73 ms, matrix size of 128×128, 10 slices of 20×20×1 mm^3 field of view (FOV), and averages (AVE) of 4 were acquired for 45 minutes following injection. K^{trans},

the contrast extravasation rate constant, maps were generated using a the Patlak model and a custom least squares curve fitting routine in MATLAB from the Gd concentration and R1 maps [67, 68].

2.5. Dihydroethidium Histological Analysis

The Pro-NP™ group was treated with Pro-NP™ in DPBS intravenously immediately after the CCI, while the MnTMPyP group was treated with a bolus injection of Mn(III)tetrakis(1-methyl-4-pyridyl)porphyrin (MnTMPyP, 475872, Sigma-Aldrich) in DPBS (500 μL of 1 mg/mL) intraperitoneally immediately after the CCI. The size of each treatment group was between 3–9 mice. A dihydroethidium (DHE, Thermo Fisher Scientific) assay was performed as previously described with modifications [6, 35, 69]. Briefly, DHE was dissolved in sterile dimethyl sulfoxide (DMSO) before further dilution in DPBS. A bolus injection of DHE (500 μL of 1.25 mg/mL, IP) was administered to each mouse at 3 h post-CCI, and mice were transcardially perfused at 1 hour after DHE injection with 4% phosphate buffered paraformaldehyde (PFA). Brain tissue was collected, fixed in 4% PFA overnight, cryoprotected in 30% sucrose, and embedded in 2.6% carboxymethylcellulose (CMC, C4888, Sigma-Aldrich). 15-μm thick slices were performed coronally on the brains utilizing a cryotome. The sections were laid on poly-L-lysine coated microscope slides (6776215, Epredia, Kalamazoo, MI), dried overnight at RT, and stored at −80 °C until use. Sections were washed thrice with DPBS and water, before mounting with ProLong™ Gold Antifade Mountant (P4981001, Thermo Fisher Scientific). Images were acquired with confocal microscopy, and quantitative fluorescence intensity analysis was performed with ImageJ software on the perilesional and the contralateral hemispheres.

2.6. Western blot

The Pro-NP™ group was treated with a bolus injection of Pro-NP™ in DPBS (9:9.8 $\times 10^3$ U SOD1:CAT/mouse, IV based on the therapeutic window results) immediately following the CCI, while the CCI group did not receive any treatment after the CCI. The control group consisted of healthy uninjured mice without any treatment. Western blot was performed as previously described with some modifications [70]. Briefly, mice were transcardially perfused at 1, 3, and 7 days post-CCI with ice-cold DPBS, and the brains were extracted. Left-right cortex and hippocampus were separated and flash-frozen in liquid nitrogen and stored at −80 °C until use. Tissues were then lysed in RIPA lysis buffer containing 1 mM phenylmethylsulfonyl fluoride. BCA assay was performed to quantify the protein concentration. For spectrin breakdown products (SBDPs), 5 μg of extract protein was resolved by 5–12% SDS-PAGE and transferred onto PVDF membranes (Bio-Rad). PVDF membranes were then washed with tris-buffered saline (TBS), blocked with 3% BLOT-*QuickBlocker*™ (G-Biosciences, St. Louis, MO) in TBS for 1 h RT, and incubated overnight at 4 °C with 1:1000 dilution of mouse anti-spectrin alpha chain (MAB1622, Sigma) and 1:1000 dilution of mouse anti-β-actin (A5441, Sigma) antibody with 3% BLOT-*QuickBlocker*™ in TTBS (0.1% v/v tween 20 in TBS). Membranes were then incubated for 1 h at room temperature with 1:5000 dilution of HRP-conjugated goat anti-mouse secondary antibody (Bio-Rad), visualized by chemiluminescence through ChemiDoc system (Clarity Western ECL Substrate, Bio-Rad), and quantified with Image Lab (Bio-Rad). For lipid peroxidation products (LPOx), 30 μg of extract protein was resolved by 10% SDS-PAGE.

The membranes were then blocked and incubated with 1:1000 dilution of rabbit anti-4-HNE (ab46545, Abcam, Cambridge, UK), 1:1000 dilution of mouse anti-acrolein (ab240918, Abcam), 1:5000 dilution of mouse anti-β-actin, and 1:3000 dilution of goat anti-rabbit or anti-mouse secondary antibody in TTBS containing 3% bovine serum albumin (BSA). 1% sodium azide was added into the blocking buffer in between different markers to deactivate the HRP, and the membrane was incubated in 1:500 dilution of goat anti-mouse IgG (ab6708, Abcam) to block the innate mouse IgG before acrolein staining. ROI was drawn on the whole lane for 4-HNE, and around 25 and 50-kDa for acrolein. Precision Plus Protein™ Dual Color Standard (1610374, Bio-Rad) was used as the protein ladder.

2.7. Statistical analysis

All the data were displayed as mean ± standard deviation. A $p < 0.05$ was considered statistically significant. The K^{trans} and DHE quantification were analyzed with one-way ANOVA and Dunnett's post hoc test against 0 h ipsilateral for K^{trans}, and untreated CCI mice for DHE. One-way ANOVA and Tukey's post hoc test was utilized for Western blot protein quantification. All statistical analysis was performed with GraphPad Prism 9 software (GraphPad Software, CA).

3. Results

3.1. Size, zeta potential, enzyme activities, and Gd concentration of Pro-NP™

Gd-Pro-NP™ had similar characterizations to our previous study [23], with r1 relaxivity at 9.4T of 5.75 s^{-1} mM^{-1}, and r2/r1 of 15. The hydrodynamic size of Pro-NP™s are in the similar range of 200–220 nm before lyophilization and 275–290 nm after lyophilization. The zeta potential of Pro-NP™ are also in the similar range of −10–25 mV. The CAT-loaded Pro-NP™ might be more anionic than the others due to the negative charge of catalase [71]. However, we did not expect difference in NPs accumulation between Pro-NP™s in the lesion since our previous study found that NPs with a surface charge from −28.8 to +13.1 mV accumulated in the brain lesion similarly [23]. Pro-NP™s showed "burst" and "sustained" releases, which were measured at 1 and 24 h in the PBS containing HSA and Tween-80 at 37 °C, as expected from a PLGA-based NP (Table 1). However, the enzyme activities *in vivo* might be higher than the enzyme activities we measured *in vitro* from released enzyme due to the diffusion of ROS into the core of NPs [72, 73]. Although Pro-NP™ was not coated with PEG, we found that Pro-NP™ are stable in the serum up to 48 h post-incubation (Supplemental Figure 1). The blood elimination half-life of Pro-NP™ was also 44.13 min in males and 56.95 min in females based on the atrial input function from the R1 mapping by MRI.

3.2. Identifying the treatment window of Gd-Pro-NP™

K^{trans} is a permeability coefficient that describes the kinetics of accumulation and retention of a contrast agent from the blood pool into tissue. We utilized K^{trans} to analyze NP transfer into injured brain lesion [23] at various time points in the acute phase of the injury (up to 24 h) (Figure 1), which can be used to evaluate the treatment window of Pro-NP™ following TBI.

There were significant reductions of Pro-NP™s accumulation in the lesion in the delayed administration compared to the immediate administration in male (mean ± SD = 32.46 ± 9.1 $\times 10^{-3}$ min^{-1}) and female (24.15 ± 12.01 $\times 10^{-3}$ min^{-1}) mice, even when administered at 1 h post-injury. Although the overall K^{trans} of males was significantly higher than females ($p < 0.01$), as determined by paired student t-test, there was no significant difference between the K^{trans} in males and females at individual time points ($p = 0.34$, 0.37, 0.32, 0.44, and 0.09 for 0, 1, 3, 6, and 24 h, respectively), as determined by student t-test. We found a significant accumulation in the lesion, compared to the contralateral hemisphere, at 24 h post-injury in male mice (6.29-fold higher, $p < 0.01$), but not in female mice (2.77-fold higher, $p = 0.12$).

3.3. Identifying the optimum SOD1:CAT-Pro-NP™ enzyme activities

With immediate injection of Gd-Pro-NP™ following a CCI (0 h time point) having the highest accumulation in the lesion, we evaluated the optimum SOD1:CAT-Pro-NP™ enzyme activities ratio and concentration in scavenging ROS when administered at this time point. *In vivo* DHE staining was utilized to measure the reduction in oxidative stress with Pro-NP™ treatment.

We found that the 4.5:4.9 and 4.5:9.8 $\times 10^3$ U/kg SOD1:CAT-Pro-NP™ ratios had the highest ROS scavenging activity following TBI (50% and 64.25% decrease, respectively). Thus, we continued with different concentrations of 4.5:4.9 $\times 10^3$ U/kg SOD1:CAT-Pro-NP™ ratio, as used in a previous study with SOD1:CAT-PLGA NP [46]. We then found that 4.5:4.9 and 9:9.8 $\times 10^3$ U/kg SOD1:CAT-Pro-NP™ showed a significant reduction in oxidative stress in male CCI mice (50% and 56.2% decrease, respectively). In female CCI mice, only 9:9.8 $\times 10^3$ U/kg SOD1:CAT-Pro-NP™ showed a significant reduction in oxidative stress (54.56% decrease). MnTMPyP, a small molecule ROS scavenger positive control, had similar efficiency in reducing ROS to the Pro-NP™ when injected immediately following the injury in male and female mice (50.66% and 65.29% decrease, respectively). Thus, we found a treatment window of 4.5:4.9 and 9:9.8 $\times 10^3$ U/kg SOD1:CAT-Pro-NP™ in male mice and 9:9.8 $\times 10^3$ U/kg SOD1:CAT-Pro-NP™ in female mice. Comparing between male and female CCI mice, we found that the untreated female CCI mice had a trending higher oxidative stress than the untreated CCI male mice ($p = 0.18$).

3.4. Time course of carbonyl stress progression in male and female mice following TBI

Finding the highest accumulation at 0 h post-injury (Figure 1) and the optimum ROS scavenging activities at 9:9.8 $\times 10^3$ U/kg SOD1:CAT-Pro-NP™ in male and female mice (Figure 2), we investigated the correlation between the reduction of ROS and the reduction of carbonyl stress following TBI by measuring 4-HNE and acrolein, two of the most prevalent LPOx aldehydes [74]. As 4-HNE and acrolein form stable covalent bonds with cysteines through thiol-Michael reaction, we measured the total volume of the LPOx-modified proteins with Western blot in the ipsi- and contralateral cortex (Supplemental Figure 2.) and hippocampus (Figure 3 & Supplemental Figure 3.). We analyzed LPOx levels at 1, 3, and 7 d post-injury since LPOx are elevated in the subacute phase of injury [75].

In the ipsilateral cortex, we found a trending reduction of 4-HNE at 1, 3, and 7 d post-injury in the Pro-NP™-treated male and female CCI mice, as well as a significant reduction of

4-HNE in the Pro-NP™-treated male CCI mice at 7 d post-injury and Pro-NP™-treated female CCI mice at 3 d post-injury, compared to the untreated CCI mice. In the ipsilateral hippocampus, we observed a significant reduction of 4-HNE in the Pro-NP™-treated male CCI mice at 1 d post-injury and the Pro-NP™-treated female CCI mice at 3 d post-injury, as well as a trending reduction of 4-HNE in the Pro-NP™-treated female CCI mice at 1 d post-injury compared to the untreated CCI mice. In the ipsilateral hippocampus, we also observed a trending reduction of acrolein with Pro-NP™ treatment at 1 d post-injury in male mice and at 3 d post-injury in female mice compared to the untreated CCI mice. In the contralateral hippocampus, we observed a trending increase of 4-HNE and acrolein at 1 d post-injury in the untreated male CCI mice, but Pro-NP™ treatment gave a trending reduction of 4-HNE compared to the untreated male CCI mice.

3.5. Time course of α-II-spectrin degradation progression in male and female mice following TBI

As we found a reduction in DHE and some reductions in LPOx with Pro-NP™ treatment following TBI, we investigated if these reductions would correlate with a reduction in cell death following TBI. α-II-spectrin breakdown products (SBDPs) have been used as a marker of necrosis and apoptosis since the size of SBDPs are dependent on the cell death pathways. SBDPs are formed through the caspase degradation pathway (apoptosis, 120kDa), calpain degradation pathway (necrosis, 145 kDa), and calpain and caspase degradation pathways (total cell death, 150 kDa) [76]. We analyzed SBDPs through Western blotting at 1, 3, and 7 d post-injury for the ipsi- and contralateral cortex and hippocampus (Figure 4) since SBDPs are most elevated in the subacute phase of injury [75].

In the ipsilateral cortex of the untreated CCI mice, we observed a significant increase in 150 kDa at 1 and 3 d post-injury in male mice, and at 1 and 7 d post-injury in female mice, compared to the control mice. We also observed a significant increase in 145 kDa at 1, 3, and 7 d post-injury in the ipsilateral cortex and hippocampus of the untreated male CCI mice compared to the control mice. In the contralateral cortex of the untreated male CCI mice, we observed a significant increase in 150 and 145 kDa at 1 d post-injury compared to the control mice. In the ipsilateral hippocampus of the untreated CCI mice, we observed a significant increase in 150 kDa at 3 d post-injury in male and female mice compared to the control mice. In the contralateral hippocampus of the untreated CCI mice, we observed a significant increase in 145 kDa at 1 and 7 d post-injury in male mice, and 150 and 145 kDa at 3 d post-injury in female mice, compared to the control mice.

We observed a significant reduction in 150 kDa with Pro-NP™ treatment at 3 d post-injury in the ipsilateral cortex of male mice, as well as bilaterally in the hippocampus of female mice, compared to the untreated CCI mice. We also observed a significant reduction in 145 kDa with Pro-NP™ treatment at 1 d post-injury bilaterally in the cortex of male mice, as well as in the contralateral hippocampus of male mice at 1 d post-injury, compared to the untreated CCI mice. However, we did not observe a significant reduction in 145 kDa with Pro-NP™ treatment in female mice compared to the untreated CCI mice. We found a significant reduction in 120 kDa with Pro-NP™ treatment in the ipsilateral hippocampus of male mice at 1 and 7 d post-injury and female mice at 3 d post-injury compared to the

untreated CCI mice. We also observed an increase in 150 kDa with Pro-NP™ treatment at 1, 3, and 7 d post-injury bilaterally in the cortex and hippocampus of male mice compared to the untreated CCI mice.

4. Discussion

There is an excess release of reactive oxygen species (ROS) immediately following TBI. The ROS oxidize DNA, lipid, and proteins, which induce more cell death and release of ROS. Mitochondrial oxidative stress damage peaks at 12 h post-injury [77], and cellular oxidative stress damage peaks around 24 h post-injury (Figure 4). Therefore, the combination of burst and sustained release of antioxidant therapies could improve the ROS scavenging activity in injury lesions at these two-time points and reduce the progression of secondary injury. In this study, we utilized Pro-NP™, an SOD1 and CAT encapsulated PLGA-based NP, with burst release within an hour of administration and sustained release for more than 24 h post-injection (Table 1) [38, 78]. PLGA NPs with similar characteristics to Pro-NP™ were almost fully retained in the spinal cord injury within one week post-administration [79], while the half-life of Gd-Pro-NP™ blood circulation was 44.13 min in males and 56.95 min in females. Although we did not study the biodistribution of Pro-NP™, we expect a similar biodistribution and clearance profile in the liver and spleen as found in an anionic PLGA NP [45]. Our finding also suggested that Pro-NP™ is stable in serum for more than 2 days (Supplemental Figure 1) even though Pro-NP™ was not PEGylated. We did not expect a significantly different accumulation and retention of SOD1-, CAT-, and Gd-Pro-NP™ in the brain lesion due to the surface charge, since previous studies did not show a significant different in the accumulation in the brain lesion and the biodistribution of NPs with surface charges ranging between −28.8 to +13.1 mV [23, 80]. Moreover, we optimized the SOD1 and CAT ratio and concentration based on the *in vivo* DHE assay at 4 h post-CCI (Figure 2). Therefore, Pro-NP™ was expected to deliver SOD1 and CAT in a similar proportion in the damaged brain for more than 24 h post-administration.

The decrease in accumulation of small molecule drugs in the brain following a TBI at later than 3 h post-injury [23] may play a role in limiting the antioxidant treatment window to 4 h post-injury, in which antioxidant treatments administered at less than 4 h post-injury showed more promising results than later administration [81]. Here, we found the highest accumulation of Gd-Pro-NP™ in the brain lesion when injected immediately following injury and with a reduction in accumulation with delayed administration of 1 h or more in both males and females (Figure 1). The downward trend of accumulation of 200 nm Gd-Pro-NP™ in the brain lesion with delayed administrations is in agreement with the 100 nm PEGylated-polystyrene NPs in a previous study by Bharadwaj et al. [19]. Although we did not find any significant difference between the K^{trans} of Gd-Pro-NP™ in male and female mice at individual time points, we found the overall K^{trans} of female mice was significantly lower than that of male mice. The lower overall K^{trans} in female mice supported previous findings that female mice have less BBB disruption in the acute phase of injury [82, 83] since BBB disruption plays a major role in the accumulation of NPs in the brain lesion [20, 25, 84]. However, an elegant study by Bharadwaj, et al. [58] found that NPs and 10–40 nm macromolecules accumulated at higher levels in females as compared to males 24 h post-injury. This difference may be a result of the size of Pro-NP™ being larger than 80

nm, which might limit accumulation in the brain lesion as compared to smaller NPs and macromolecules that can more freely diffuse through vascular occlusions into the brain parenchyma and neurons [84]. Overall, these findings suggest there are important size and material effects, which impacted the lesion accumulation differently in males and females and need to be further explored.

Establishing a therapeutic window for antioxidant treatments is particularly important because of the bell-shaped efficacy curve [85–87]. Suboptimal dosing of antioxidants was found to reduce the effectiveness of antioxidants treatment [26, 86–89]. SOD1 was also found to aggravate the injury when administered at higher than 10,000 U/kg SOD1 in a ischemia-reperfusion injury study [47] and higher than 20,000 U/kg SOD1 in the heart reoxygenation studies [85]. However, the optimal doses and ratio of SOD1- and CAT-Pro-NP™ for TBI has not been established. Therefore, the therapeutic window of Pro-NP™ was studied here to give the best performance in reducing oxidative stress following TBI. We found that 4.5:4.9, 4.5:9.8, and 9:9.8 $\times 10^3$ U/kg SOD1:CAT-Pro-NP™ treatment gave the largest reduction in ROS, while 8,500 U/kg SOD1-Pro-NP™ and 4,100 U/kg CAT-Pro-NP™ treatment groups did not show a significant decrease in oxidative stress compared to the untreated CCI mice (Figure 2). The results suggested that the combination of SOD1 and CAT gave higher efficacy than the separate treatment of SOD1 or CAT treatment because scavenging superoxide ($O_2^{\bullet -}$) with SOD1 may produce excess H_2O_2, which fuels the Fenton reaction. Administering CAT without SOD1 may also be limited by the availability of H_2O_2 from $O_2^{\bullet -}$. We chose 9:9.8 $\times 10^3$ SOD1:CAT-Pro-NP™ for a ratio similar to PLGA NPs for spinal cord injury [46], and similar concentration to 10,000 U/kg SOD1 and 10,000 U/kg CAT, which are the common dosages used in preclinical studies and clinical trials [10, 11, 13, 47, 90–92]. Here, we found that the untreated female CCI mice had a trending higher oxidative stress than the untreated male CCI mice ($p = 0.18$), which might be correlated with higher IL-1β and TNFα cytokine expression, as well as higher pro-inflammatory markers and apoptosis level, in females at 4 h post-injury [57]. However, at 1 and 3 days post-injury, female CCI mice have less pro-inflammatory markers, astrogliosis, microglia activation, and macrophage infiltration, which might lead to lower levels of apoptosis and smaller lesion areas [56, 57]. Moreover, female mice have higher endogenous antioxidant enzyme activities in the brain [93–96], which may lead to better outcomes for female mice following a moderate-severe CCI [57, 63, 97–100]. Thus, our observed higher ROS in female CCI mice in the acute phase is likely compensated by a higher expression of endogenous antioxidant enzymes. In this study, we also did not look at the effect of SOD- and CAT-Pro-NP™ individually as we focused on identifying the most effective ratio and concentration of SOD- and CAT-Pro-NP™ in reducing the secondary injury. Individual treatment groups of SOD- and CAT-Pro-NP™ may give a better understanding of the role of $O_2^{\bullet -}$ and H_2O_2 in TBI, since $O_2^{\bullet -}$ and H_2O_2 may induce different signaling cascade in the brain tissue [101–103]. A separate SOD- and CAT-NP treatments for brain injury have also been studied previously [47–49, 69].

Lipid peroxidation products (LPOx) are reactive downstream products of lipids oxidized by ROS [104]. 4-HNE and acrolein are two of the most abundant and reactive LPOx aldehydes. The alkene and aldehyde functional groups of 4-HNE and acrolein readily form covalent bonds with cysteine and lysine of proteins, respectively. Here we found that the LPOx in

the untreated CCI mice peaked at 1–3 d post-injury (Figure 3 and Supplemental Figure 2 and 3). From the trending reductions of 4-HNE and acrolein bilaterally in the cortex and hippocampus at 1 and 3 d post-injury, our results suggest that Pro-NP™ scavenged ROS in the primary injury and provided some ROS scavenging activities up to 3 d post-injury, due to the sustained release and retention half-life in the damaged brain parenchyma of more than 24 h post-administration [26, 79, 86, 105]. Previous studies did not find a significant increase in LPOx in the contralateral cortex and hippocampus [97, 106]. However, we found a significant increase in acrolein at 3 d post-injury in the contralateral hippocampus of male mice. The increase in acrolein in the contralateral hippocampus of male mice at 1 and 3 d post-injury might suggest the spread of oxidative stress from the severe CCI injury into the contralateral hippocampus. We also observed a delay in the elevation of acrolein in the contralateral hemisphere of female mice from 1 d to 3 d post-injury, which might be due to higher reduced glutathione (GSH) [94], glutathione-S-transferase [95], and catalase [93, 96] activities in the brain of female mice, which delayed the spread of ROS into the contralateral hemisphere, as was mimicked with Pro-NP™ treatment in male mice in the contralateral hippocampus. Our results suggest that although additional ROS scavengers can be beneficial in the ipsilateral hemisphere at 1 and 3 d post-injury, there might be a threshold of ROS scavengers needed to limit the spread of ROS into the contralateral hemisphere.

Calpain and caspase-3 are drivers of the necrosis and apoptosis cell death pathways, respectively. Calpain and caspase-3 are activated by elevated intracellular Ca^{2+}. Calpain and caspase-3 also degrade the neuronal cytoskeleton filament α-II-spectrin into α-II-spectrin breakdown products (SBDPs) through two separate pathways [107, 108]. In the ipsilateral hemisphere of the untreated CCI mice, SBDPs peaked at 1–3 d post-injury (Figure 4). Although Pro-NP™ treatment did not reduce necrosis in the ipsilateral hippocampus of male and female mice, we observed a significant reduction of apoptosis at 1 and 7 d post-injury in male mice and a trending reduction of apoptosis at 3 d post-injury in female mice. This suggests that the injury was too severe for Pro-NP™ to reduce necrosis, but Pro-NP™ provided protection against apoptosis in the ipsilateral hippocampus, especially in male mice. Previous studies did not find a significant increase in SBDPs in the contralateral hemisphere following TBI [109–112], but we found a significant increase in SBDPs that peaked at 1 d post-injury in the contralateral cortex and hippocampus of male mice and 3 d post-injury in the contralateral hippocampus of female mice. The significant increase of SBDPs we observed in the contralateral hemisphere might be caused by the severe CCI we utilized in this study, as well as the use of a mouse model of TBI rather than a rat model of TBI that was employed in the previous studies. We found a delay in the increase of necrosis in the contralateral cortex and hippocampus in female CCI mice compared to male CCI mice. Higher endogenous antioxidant enzyme activities in the brain of female than male mice [93–96] may cause the delay of cell death in the contralateral hemisphere in female mice, which was mimicked by the Pro-NP™ treatment in male CCI mice. In the contralateral hemisphere of the Pro-NP™ treated female CCI mice, we did not observe any reduction of necrosis at 3 d post-injury compared to the untreated female CCI mice. However, we found a significant reduction in total cell death in the contralateral hippocampus and trending reductions in apoptosis at 3 d post-injury in the contralateral cortex and hippocampus of the Pro-NP™-treated female CCI mice compared to the untreated female CCI mice. This

suggests some, but not significant, protection from Pro-NP™ treatment in the female CCI mice in reducing the spread of ROS into the contralateral hemisphere in the acute phase of injury. For future development, antioxidant NPs like Pro-NP™ may also be beneficial for various other diseases with elevated ROS production, such as ischemia, neurodegeneration, cardiovascular, respiratory, and cancer [119–122].

A possible limitation of this study is that Pro-NP™ may not have provided sufficient antioxidant enzyme activity to achieve a significant therapeutic benefit in the subacute phase of injury even though the therapeutic dose of SOD1:CAT Pro-NP™ was optimized in the acute phase of injury (Figure 2). In the subacute phase of injury, we found a delay in the elevation of 4-HNE and acrolein the ipsilateral hippocampus, acrolein in the contralateral hippocampus, and 145 kDa SBDP in the contralateral cortex and hippocampus, of Pro-NP™-treated male CCI mice at 3 d post-injury compared to 1 d post-injury in the untreated male CCI mice. In the future, increasing the sustained release rate in the damaged brain parenchyma may improve the therapeutic effect of Pro-NP™ in reducing LPOx and SBDPs in the subacute and chronic phases of injury. Utilizing active targeting to increase Pro-NP™ accumulation in the subacute phase of injury might also be a feasible improvement to afford protection into the chronic phase of injury. For example, intracellular cell adhesion molecule 1 (ICAM1) was found to be overexpressed following a TBI, which improved the delivery and target engagement of anti-ICAM1 conjugated with antioxidant enzymes [69, 113, 114] and NPs conjugated with anti-ICAM1 [113, 115, 116]. Conjugating folate or anti-PECAM-1 antibody on the surface of Pro-NP™ may also improve the delivery of SOD and CAT by promoting the uptake of Pro-NP™ through the caveolin pathway [117, 118]. Overall, we observed that Pro-NP™ treatment benefited male mice more than female mice in reducing post-traumatic markers of oxidative stress. Without Pro-NP™ treatment, male mice showed elevlated markers of post-traumatic oxidative stress in the contralateral hemisphere whereas untreated female mice and males treated with Pro-NP™ did not show these elevated levels. Female mice, which have higher endogenous levels of antioxidant enzymes, might have sufficient ROS scavenging activities to limit the progression of secondary injury to the contralateral hemisphere whereas male mice required the input of exogenous antioxidant enzymes through Pro-NP™ treatment. This suggests there may be a threshold of ROS scavenging activities needed to reduce this secondary spread since female mice treated with Pro-NP™ did not receive an additional benefit. Therefore, multiple therapeutic targets, such as LPOx and inflammation, are likely required in addition to ROS to reduce the secondary spread of injury following TBI and improve outcomes in both males and females. It is a possibility that the sex-based differences we observed were solely a consequence of size differences between males and females. Although this study was not designed and statistically powered for comparing sex-based size differences, we optimized the treatment time point and dosing for males and females separately to best control for possible size-based differences since the optimal dose identified was based on size (i.e., 9:9.8 $\times 10^3$ U/kg). We also utilized robust analysis methods, such as K^{trans}, that are not sensitive to size differences; thus, we strongly believe these sex-based findings are not confounded by size differences.

5. Conclusion

Excess ROS is released following TBI that can spread and induce a cascade of secondary injury. An antioxidant NP with burst and sustained release of SOD1 and CAT, as well as high accumulation and retention in the injured brain, was utilized in this study. Pro-NP™ accumulated in the damaged brain parenchyma at the highest level when administered immediately after injury, and the accumulation was significantly reduced with delayed administration of 1 h or more. We found the overall accumulation of Pro-NP™ in the brain lesion was higher in male than in female mice, which suggested less BBB disruption in female mice. We found higher ROS levels in the untreated female CCI mice as compared to the untreated male CCI mice, and 9:9.8 $\times 10^3$ SOD1:CAT-Pro-NP™ treatment gave the highest reduction in oxidative stress in both male and female mice. Higher endogenous antioxidant activities in female mice might have delayed the increase in post-traumatic markers of oxidative stress (LPOx and SPDPs) in the contralateral hemisphere to 3 d post-injury compared to 1 d post-injury in male mice. The delayed elevation of post-traumatic markers of oxidative stress in the contralateral hemisphere of female mice was mimicked with Pro-NP™ treatment in male mice. Thus, there appear to be important sex-based differences in response to antioxidant NP delivery. Our results also suggest that there is a maximum threshold of ROS scavengers for TBI therapy beyond which no additional benefit is observed, which underscores the need for multiple treatment targets to mitigate the progression of secondary injury.

Supplementary Material

Refer to Web version on PubMed Central for supplementary material.

ACKNOWLEDGMENTS

We acknowledge grant funding from the National Institute of Neurological Disorders and Stroke of the National Institutes of Health R01NS109488 to F.K. and R41NS119082 to F.K. and G.M. This material is based upon work supported by the National Science Foundation Graduate Research Fellowship under the grant no. DGE-1610400 to H.M. This investigation is solely the responsibility of the authors and does not necessarily represent the official views of NINDS, NIH, and NSF. We acknowledge the Nano-Engineering Research Core facility supported by Nebraska Research Initiative fund for use of the confocal microscope.

References

[1]. Aleman M, Prange T, Neurocranium and Brain, in: Equine Surgery, 2019, pp. 895–900.

[2]. Johnson VE, Stewart JE, Begbie FD, Trojanowski JQ, Smith DH, Stewart W, Inflammation and white matter degeneration persist for years after a single traumatic brain injury, Brain, 136 (2013) 28–42. [PubMed: 23365092]

[3]. Leconte C, Benedetto C, Lentini F, Simon K, Ouaazizi C, Taib T, Cho AH, Plotkine M, Mongeau R, Marchand-Leroux C, Besson VC, Histological and behavioral evaluation after traumatic brain injury in mice: a ten months follow-up study, J Neurotrauma, (2019).

[4]. Mao X, Terpolilli NA, Wehn A, Chen S, Hellal F, Liu B, Seker B, Plesnila N, Progressive histopathological damage occurring up to one year after experimental traumatic brain injury is associated with cognitive decline and depression-like behavior, J Neurotrauma, (2019).

[5]. Janatpour ZC, Korotcov A, Bosomtwi A, Dardzinski BJ, Symes AJ, Subcutaneous Administration of Angiotensin-(1–7) Improves Recovery after Traumatic Brain Injury in Mice, Journal of Neurotrauma, 36 (2019) 3115–3131. [PubMed: 31037999]

[6]. Tarudji AW, Gee CC, Romereim SM, Convertine AJ, Kievit FM, Antioxidant thioether core-crosslinked nanoparticles prevent the bilateral spread of secondary injury to protect spatial learning and memory in a controlled cortical impact mouse model of traumatic brain injury, Biomaterials, 272 (2021) 120766. [PubMed: 33819812]

[7]. Niu X, Zheng S, Liu H, Li S, Protective effects of taurine against inflammation, apoptosis, and oxidative stress in brain injury, Molecular Medicine Reports, (2018).

[8]. Liang J, Wu S, Xie W, He H, Ketamine ameliorates oxidative stress-induced apoptosis in experimental traumatic brain injury via the Nrf2 pathway, Drug Design, Development and Therapy, Volume 12 (2018) 845–853.

[9]. Bailey ZS, Nilson E, Bates JA, Oyalowo A, Hockey KS, Sajja VSSS, Thorpe C, Rogers H, Dunn B, Frey AS, Billings MJ, Sholar CA, Hermundstad A, Kumar C, VandeVord PJ, Rzigalinski BA, Cerium Oxide Nanoparticles Improve Outcome after In Vitro and In Vivo Mild Traumatic Brain Injury, Journal of Neurotrauma, 37 (2020) 1452–1462. [PubMed: 27733104]

[10]. Liu TH, Beckman JS, Freeman BA, Hogan EL, Hsu CY, Polyethylene glycol-conjugated superoxide dismutase and catalase reduce ischemic brain injury, American Journal of Physiology-Heart and Circulatory Physiology, 256 (1989) H589–H593.

[11]. Muizelaar JP, Clinical trials with Dismutec (pegorgotein; polyethylene glycol-conjugated superoxide dismutase; PEG-SOD) in the treatment of severe closed head injury, Adv Exp Med Biol, 366 (1994) 389–400. [PubMed: 7771267]

[12]. Muizelaar JP, Kupiec JW, Rapp LA, PEG-SOD after head injury, J Neurosurg, 83 (1995) 942.

[13]. Muizelaar JP, Marmarou A, Young HF, Choi SC, Wolf A, Schneider RL, Kontos HA, Improving the outcome of severe head injury with the oxygen radical scavenger polyethylene glycol-conjugated superoxide dismutase: a phase II trial, J Neurosurg, 78 (1993) 375–382. [PubMed: 8433137]

[14]. Hatton J, Rosbolt B, Empey P, Kryscio R, Young B, Dosing and safety of cyclosporine in patients with severe brain injury, Journal of Neurosurgery, 109 (2008) 699–707. [PubMed: 18826358]

[15]. Marshall LF, Maas AIR, Marshall SB, Bricolo A, Fearnside M, Iannotti F, Klauber MR, Lagarrigue J, Lobato R, Persson L, Pickard JD, Piek J, Servadei F, Wellis GN, Morris GF, Means ED, Musch B, A multicenter trial on the efficacy of using tirilazad mesylate in cases of head injury, Journal of Neurosurgery, 89 (1998) 519–525. [PubMed: 9761043]

[16]. Hoffer ME, Balaban C, Slade MD, Tsao JW, Hoffer B, Amelioration of acute sequelae of blast induced mild traumatic brain injury by N-acetyl cysteine: a double-blind, placebo controlled study, PLoS One, 8 (2013) e54163. [PubMed: 23372680]

[17]. Miller SM, Zynda AJ, Sabatino MJ, Jo C, Ellis HB, Dimeff RJ, A Pilot Randomized Controlled Trial of Docosahexaenoic Acid for the Treatment of Sport-Related Concussion in Adolescents, Clin Pediatr (Phila), 61 (2022) 785–794. [PubMed: 35722886]

[18]. McPherson RA, Mangram AJ, Barletta JF, Dzandu JK, N -acetylcysteine is associated with reduction of postconcussive symptoms in elderly patients: A pilot study, J Trauma Acute Care Surg, 93 (2022) 644–649. [PubMed: 35393384]

[19]. Bharadwaj VN, Lifshitz J, Adelson PD, Kodibagkar VD, Stabenfeldt SE, Temporal assessment of nanoparticle accumulation after experimental brain injury: Effect of particle size, Sci Rep, 6 (2016) 29988. [PubMed: 27444615]

[20]. Bharadwaj VN, Rowe RK, Harrison J, Wu C, Anderson TR, Lifshitz J, Adelson PD, Kodibagkar VD, Stabenfeldt SE, Blood-brainbarrier disruption dictates nanoparticle accumulation following experimental brain injury, Nanomedicine, 14 (2018) 2155–2166. [PubMed: 29933022]

[21]. Bony BA, Miller HA, Tarudji AW, Gee CC, Sarella A, Nichols MG, Kievit FM, Ultrasmall Mixed Eu-Gd Oxide Nanoparticles for Multimodal Fluorescence and Magnetic Resonance Imaging of Passive Accumulation and Retention in TBI, ACS Omega, 5 (2020) 16220–16227. [PubMed: 32656444]

[22]. Cruz LJ, Stammes MA, Que I, van Beek ER, Knol-Blankevoort VT, Snoeks TJA, Chan A, Kaijzel EL, Löwik CWGM, Effect of PLGA NP size on efficiency to target traumatic brain injury, Journal of Controlled Release, 223 (2016) 31–41. [PubMed: 26708021]

[23]. Miller HA, Magsam AW, Tarudji AW, Romanova S, Weber L, Gee CC, Madsen GL, Bronich TK, Kievit FM, Evaluating differential nanoparticle accumulation and retention kinetics in a mouse

model of traumatic brain injury via Ktrans mapping with MRI, Scientific Reports, 9 (2019) 16099. [PubMed: 31695100]

[24]. Xu JL, Ypma M, Chiarelli PA, Park J, Ellenbogen RG, Stayton PS, Mourad PD, Lee D, Convertine AJ, Kievit FM, Theranostic Oxygen Reactive Polymers for Treatment of Traumatic Brain Injury, Adv Funct Mater, 26 (2016) 4124–4133.

[25]. Boyd BJ, Galle A, Daglas M, Rosenfeld JV, Medcalf R, Traumatic brain injury opens blood–brain barrier to stealth liposomes via an enhanced permeability and retention (EPR)-like effect, Journal of Drug Targeting, 23 (2015) 847–853. [PubMed: 26079716]

[26]. Bailey ZS, Nilson E, Bates JA, Oyalowo A, Hockey KS, Sajja V, Thorpe C, Rogers H, Dunn B, Frey AS, Billings MJ, Sholar CA, Hermundstad A, Kumar C, VandeVord PJ, Rzigalinski BA, Cerium Oxide Nanoparticles Improve Outcome after In Vitro and In Vivo Mild Traumatic Brain Injury, J Neurotrauma, 37 (2020) 1452–1462. [PubMed: 27733104]

[27]. Han Z, Han Y, Huang X, Ma H, Zhang X, Song J, Dong J, Li S, Yu R, Liu H, A Novel Targeted Nanoparticle for Traumatic Brain Injury Treatment: Combined Effect of ROS Depletion and Calcium Overload Inhibition, Advanced Healthcare Materials, (2022).

[28]. Li Q, Gao Y, Shen J, Mu X, Wang J, Ouyang L, Chen K, He H, Pei J, Ren Q, Sun S, Liu H, Zhou L, Sun Y, Long W, Zhang J, Zhang X-D, Catalase-like quantum dots of l-lysine polymerization as free radical scavengers for hypoxic brain injury, Materials Today Communications, 27 (2021).

[29]. Mu X, He H, Wang J, Long W, Li Q, Liu H, Gao Y, Ouyang L, Ren Q, Sun S, Wang J, Yang J, Liu Q, Sun Y, Liu C, Zhang X-D, Hu W, Carbogenic Nanozyme with Ultrahigh Reactive Nitrogen Species Selectivity for Traumatic Brain Injury, Nano Letters, 19 (2019) 4527–4534. [PubMed: 31244237]

[30]. Ouyang L, Mu X, Wang J, Li Q, Gao Y, Liu H, Sun S, Ren Q, Yan R, Wang J, Liu Q, Sun Y, Liu C, He H, Long W, Zhang X-D, Carbon dot targeting to nitrogen signaling molecules for inhibiting neuronal death, Journal of Materials Chemistry B, 8 (2020) 2321–2330. [PubMed: 32100792]

[31]. Sharma A, Liaw K, Sharma R, Zhang Z, Kannan S, Kannan RM, Targeting Mitochondrial Dysfunction and Oxidative Stress in Activated Microglia using Dendrimer-Based Therapeutics, Theranostics, 8 (2018) 5529–5547. [PubMed: 30555562]

[32]. Takahashi T, Marushima A, Nagasaki Y, Hirayama A, Muroi A, Puentes S, Mujagic A, Ishikawa E, Matsumura A, Novel neuroprotection using antioxidant nanoparticles in a mouse model of head trauma, Journal of Trauma and Acute Care Surgery, 88 (2020) 677–685. [PubMed: 32039974]

[33]. Yoo D, Magsam AW, Kelly AM, Stayton PS, Kievit FM, Convertine AJ, Core-Cross-Linked Nanoparticles Reduce Neuroinflammation and Improve Outcome in a Mouse Model of Traumatic Brain Injury, Acs Nano, 11 (2017) 8600–8611. [PubMed: 28783305]

[34]. Youn DH, Tran NM, Kim BJ, Kim Y, Jeon JP, Yoo H, Shape effect of cerium oxide nanoparticles on mild traumatic brain injury, Scientific Reports, 11 (2021).

[35]. Priester A, Waters R, Abbott A, Hilmas K, Woelk K, Miller HA, Tarudji AW, Gee CC, McDonald B, Kievit FM, Convertine AJ, Theranostic Copolymers Neutralize Reactive Oxygen Species and Lipid Peroxidation Products for the Combined Treatment of Traumatic Brain Injury, Biomacromolecules, 23 (2022) 1703–1712. [PubMed: 35316025]

[36]. Petkau A, Chelack WS, Kelly K, Barefoot C, Monasterski L, Tissue distribution of bovine 125I-superoxide dismutase in mice, Res Commun Chem Pathol Pharmacol, 15 (1976) 641–654. [PubMed: 1005912]

[37]. Odlind B, Appelgren LE, Bayati A, Wolgast M, Tissue distribution of 125I-labelled bovine superoxide dismutase (SOD) in the rat, Pharmacol Toxicol, 62 (1988) 95–100. [PubMed: 3353358]

[38]. Labhasetwar Vinod D, Compositions and methods for the treatment of photoaging and other conditions, in, PRO TRANSIT NANOTHERAPY LLC PROTRANSIT NANOTHERAPY LLC, US, 2019.

[39]. Galliani M, Tremolanti C, Signore G, Nanocarriers for Protein Delivery to the Cytosol: Assessing the Endosomal Escape of Poly(Lactide-co-Glycolide)-Poly(Ethylene Imine) Nanoparticles, Nanomaterials, 9 (2019).

[40]. Hood ED, Chorny M, Greineder CF, Alferiev IS, Levy RJ, Muzykantov VR, Endothelial targeting of nanocarriers loaded with antioxidant enzymes for protection against vascular oxidative stress and inflammation, Biomaterials, 35 (2014) 3708–3715. [PubMed: 24480537]

[41]. Howard MD, Hood ED, Greineder CF, Alferiev IS, Chorny M, Muzykantov V, Targeting to Endothelial Cells Augments the Protective Effect of Novel Dual Bioactive Antioxidant/Anti-Inflammatory Nanoparticles, Molecular Pharmaceutics, 11 (2014) 2262–2270. [PubMed: 24877560]

[42]. Chorny M, Hood E, Levy RJ, Muzykantov VR, Endothelial delivery of antioxidant enzymes loaded into non-polymeric magnetic nanoparticles, Journal of Controlled Release, 146 (2010) 144–151. [PubMed: 20483366]

[43]. Shuvaev VV, Khoshnejad M, Pulsipher KW, Kiseleva RY, Arguiri E, Cheung-Lau JC, LeFort KM, Christofidou-Solomidou M, Stan RV, Dmochowski IJ, Muzykantov VR, Spatially controlled assembly of affinity ligand and enzyme cargo enables targeting ferritin nanocarriers to caveolae, Biomaterials, 185 (2018) 348–359. [PubMed: 30273834]

[44]. Kim M-S, Stees M, Karuturi BVK, Vijayaraghavalu S, Peterson RE, Madsen GL, Labhasetwar V, Pro-NP™ protect against TiO2 nanoparticle-induced phototoxicity in zebrafish model: exploring potential application for skin care, Drug Delivery and Translational Research, 7 (2017) 372–382. [PubMed: 28299721]

[45]. Adjei IM, Peetla C, Labhasetwar V, Heterogeneity in nanoparticles influences biodistribution and targeting, Nanomedicine, 9 (2014) 267–278. [PubMed: 23799984]

[46]. Andrabi SS, Yang J, Gao Y, Kuang Y, Labhasetwar V, Nanoparticles with antioxidant enzymes protect injured spinal cord from neuronal cell apoptosis by attenuating mitochondrial dysfunction, Journal of Controlled Release, 317 (2020) 300–311. [PubMed: 31805339]

[47]. Reddy MK, Labhasetwar V, Nanoparticle-mediated delivery of superoxide dismutase to the brain: an effective strategy to reduce ischemia-reperfusion injury, The FASEB Journal, 23 (2009) 1384–1395. [PubMed: 19124559]

[48]. Reddy MK, Wu L, Kou W, Ghorpade A, Labhasetwar V, Superoxide Dismutase-Loaded PLGA Nanoparticles Protect Cultured Human Neurons Under Oxidative Stress, Applied Biochemistry and Biotechnology, 151 (2008) 565–577. [PubMed: 18509606]

[49]. Singhal A, Morris VB, Labhasetwar V, Ghorpade A, Nanoparticle-mediated catalase delivery protects human neurons from oxidative stress, Cell Death Dis, 4 (2013) e903. [PubMed: 24201802]

[50]. Mair O, Greve F, Lefering R, Biberthaler P, Hanschen M, TraumaRegister DGU, The outcome of severely injured patients following traumatic brain injury is affected by gender-A retrospective, multicenter, matched-pair analysis utilizing data of the TraumaRegister DGU((R)), Front Neurosci, 16 (2022) 974519. [PubMed: 36340759]

[51]. Gupte RP, Brooks WM, Vukas RR, Pierce JD, Harris JL, Sex Differences in Traumatic Brain Injury: What We Know and What We Should Know, Journal of Neurotrauma, 36 (2019) 3063–3091. [PubMed: 30794028]

[52]. Goldstein FC, Caveney AF, Hertzberg VS, Silbergleit R, Yeatts SD, Palesch YY, Levin HS, Wright DW, Very Early Administration of Progesterone Does Not Improve Neuropsychological Outcomes in Subjects with Moderate to Severe Traumatic Brain Injury, J Neurotrauma, 34 (2017) 115–120. [PubMed: 26973025]

[53]. Kalimon OJ, Sullivan PG, Sex Differences in Mitochondrial Function Following a Controlled Cortical Impact Traumatic Brain Injury in Rodents, Front Mol Neurosci, 14 (2021) 753946. [PubMed: 34720875]

[54]. Svedung Wettervik T, Hanell A, Howells T, Enblad P, Lewen A, Females Exhibit Better Cerebral Pressure Autoregulation, Less Mitochondrial Dysfunction, and Reduced Excitotoxicity after Severe Traumatic Brain Injury, J Neurotrauma, 39 (2022) 1507–1517. [PubMed: 35587145]

[55]. Greco T, Vespa PM, Prins ML, Alternative substrate metabolism depends on cerebral metabolic state following traumatic brain injury, Exp Neurol, 329 (2020) 113289. [PubMed: 32247790]

[56]. Doran SJ, Ritzel RM, Glaser EP, Henry RJ, Faden AI, Loane DJ, Sex Differences in Acute Neuroinflammation after Experimental Traumatic Brain Injury Are Mediated by Infiltrating Myeloid Cells, Journal of Neurotrauma, 36 (2019) 1040–1053. [PubMed: 30259790]

[57]. Villapol S, Loane DJ, Burns MP, Sexual dimorphism in the inflammatory response to traumatic brain injury, Glia, 65 (2017) 1423–1438. [PubMed: 28608978]

[58]. Bharadwaj VN, Copeland C, Mathew E, Newbern J, Anderson TR, Lifshitz J, Kodibagkar VD, Stabenfeldt SE, Sex-Dependent Macromolecule and Nanoparticle Delivery in Experimental Brain Injury, Tissue Eng Part A, 26 (2020) 688–701. [PubMed: 32697674]

[59]. Petersen A, Soderstrom M, Saha B, Sharma P, Animal models of traumatic brain injury: a review of pathophysiology to biomarkers and treatments, Exp Brain Res, 239 (2021) 2939–2950. [PubMed: 34324019]

[60]. McDonald BZ, Gee CC, Kievit FM, The Nanotheranostic Researcher's Guide for Use of Animal Models of Traumatic Brain Injury, Journal of Nanotheranostics, 2 (2021) 224–268. [PubMed: 35655793]

[61]. Bramlett HM, Dietrich WD, Neuropathological Protection after Traumatic Brain Injury in Intact Female Rats Versus Males or Ovariectomized Females, Journal of Neurotrauma, 18 (2001) 891–900. [PubMed: 11565601]

[62]. Monaco CM, Mattiola VV, Folweiler KA, Tay JK, Yelleswarapu NK, Curatolo LM, Matter AM, Cheng JP, Kline AE, Environmental enrichment promotes robust functional and histological benefits in female rats after controlled cortical impact injury, Exp Neurol, 247 (2013) 410–418. [PubMed: 23333563]

[63]. Tucker LB, Fu AH, McCabe JT, Performance of Male and Female C57BL/6J Mice on Motor and Cognitive Tasks Commonly Used in Pre-Clinical Traumatic Brain Injury Research, Journal of Neurotrauma, 33 (2016) 880–894. [PubMed: 25951234]

[64]. Tucker LB, Burke JF, Fu AH, McCabe JT, Neuropsychiatric Symptom Modeling in Male and Female C57BL/6J Mice after Experimental Traumatic Brain Injury, Journal of Neurotrauma, 34 (2017) 890–905. [PubMed: 27149139]

[65]. Deoni SC, Rutt BK, Peters TM, Rapid combined T1 and T2 mapping using gradient recalled acquisition in the steady state, Magn Reson Med, 49 (2003) 515–526. [PubMed: 12594755]

[66]. Deoni SC, Peters TM, Rutt BK, High-resolution T1 and T2 mapping of the brain in a clinically acceptable time with DESPOT1 and DESPOT2, Magn Reson Med, 53 (2005) 237–241. [PubMed: 15690526]

[67]. Patlak CS, Blasberg RG, Graphical Evaluation of Blood-to-Brain Transfer Constants from Multiple-Time Uptake Data. Generalizations, Journal of Cerebral Blood Flow & Metabolism, 5 (1985) 584–590. [PubMed: 4055928]

[68]. Tofts PS, Brix G, Buckley DL, Evelhoch JL, Henderson E, Knopp MV, Larsson HB, Lee TY, Mayr NA, Parker GJ, Port RE, Taylor J, Weisskoff RM, Estimating kinetic parameters from dynamic contrast-enhanced T(1)-weighted MRI of a diffusable tracer: standardized quantities and symbols, J Magn Reson Imaging, 10 (1999) 223–232. [PubMed: 10508281]

[69]. Lutton EM, Razmpour R, Andrews AM, Cannella LA, Son Y-J, Shuvaev VV, Muzykantov VR, Ramirez SH, Acute administration of catalase targeted to ICAM-1 attenuates neuropathology in experimental traumatic brain injury, Scientific Reports, 7 (2017).

[70]. Bony BA, Tarudji AW, Miller HA, Gowrikumar S, Roy S, Curtis ET, Gee CC, Vecchio A, Dhawan P, Kievit FM, Claudin-1-Targeted Nanoparticles for Delivery to Aging-Induced Alterations in the Blood-Brain Barrier, Acs Nano, (2021).

[71]. Feoktistova NA, Vikulina AS, Balabushevich NG, Skirtach AG, Volodkin D, Bioactivity of catalase loaded into vaterite CaCO3 crystals via adsorption and co-synthesis, Materials & Design, 185 (2020).

[72]. Simone EA, Dziubla TD, Colon-Gonzalez F, Discher DE, Muzykantov VR, Effect of polymer amphiphilicity on loading of a therapeutic enzyme into protective filamentous and spherical polymer nanocarriers, Biomacromolecules, 8 (2007) 3914–3921. [PubMed: 18038999]

[73]. Dziubla TD, Shuvaev VV, Hong NK, Hawkins BJ, Madesh M, Takano H, Simone E, Nakada MT, Fisher A, Albelda SM, Muzykantov VR, Endothelial targeting of semipermeable polymer nanocarriers for enzyme therapies, Biomaterials, 29 (2008) 215–227. [PubMed: 17950837]

[74]. Esterbauer H, Schaur RJ, Zollner H, Chemistry and biochemistry of 4-hydroxynonenal, malonaldehyde and related aldehydes, Free Radical Biology and Medicine, 11 (1991) 81–128. [PubMed: 1937131]

[75]. Hill RL, Singh IN, Wang JA, Hall ED, Time courses of post-injury mitochondrial oxidative damage and respiratory dysfunction and neuronal cytoskeletal degradation in a rat model of focal traumatic brain injury, Neurochemistry International, 111 (2017) 45–56. [PubMed: 28342966]

[76]. Wang KKW, Posmantur R, Nath R, McGinnis K, Whitton M, Talanian RV, Glantz SB, Morrow JS, Simultaneous Degradation of αII- and βII-Spectrin by Caspase 3 (CPP32) in Apoptotic Cells, Journal of Biological Chemistry, 273 (1998) 22490–22497. [PubMed: 9712874]

[77]. Singh IN, Sullivan PG, Deng Y, Mbye LH, Hall ED, Time Course of Post-Traumatic Mitochondrial Oxidative Damage and Dysfunction in a Mouse Model of Focal Traumatic Brain Injury: Implications for Neuroprotective Therapy, Journal of Cerebral Blood Flow & Metabolism, 26 (2006) 1407–1418. [PubMed: 16538231]

[78]. Labhasetwar Vinod D, Reddy Maram K, Method and composition for inhibiting reperfusion injury in the brain, in, LABHASETWAR VINOD D REDDY MARAM K, US, 2006.

[79]. Gao Y, Vijayaraghavalu S, Stees M, Kwon BK, Labhasetwar V, Evaluating accessibility of intravenously administered nanoparticles at the lesion site in rat and pig contusion models of spinal cord injury, Journal of Controlled Release, 302 (2019) 160–168. [PubMed: 30930216]

[80]. Xiao K, Li Y, Luo J, Lee JS, Xiao W, Gonik AM, Agarwal RG, Lam KS, The effect of surface charge on in vivo biodistribution of PEG-oligocholic acid based micellar nanoparticles, Biomaterials, 32 (2011) 3435–3446. [PubMed: 21295849]

[81]. Mohamadpour M, Whitney K, Bergold PJ, The Importance of Therapeutic Time Window in the Treatment of Traumatic Brain Injury, Front Neurosci, 13 (2019) 07. [PubMed: 30728762]

[82]. O'Connor CA, Cernak I, Vink R, The temporal profile of edema formation differs between male and female rats following diffuse traumatic brain injury, Acta Neurochir Suppl, 96 (2006) 121–124. [PubMed: 16671438]

[83]. Hubbard WB, Velmurugan GV, Brown EP, Sullivan PG, Resilience of females to acute blood–brain barrier damage and anxiety behavior following mild blast traumatic brain injury, Acta Neuropathologica Communications, 10 (2022).

[84]. Khalin I, Adarsh N, Schifferer M, Wehn A, Groschup B, Misgeld T, Klymchenko A, Plesnila N, Size-Selective Transfer of Lipid Nanoparticle-Based Drug Carriers Across the Blood Brain Barrier Via Vascular Occlusions Following Traumatic Brain Injury, Small, 18 (2022).

[85]. McCord JM, Superoxide dismutase, lipid peroxidation, and bell-shaped dose response curves, Dose Response, 6 (2008) 223–238. [PubMed: 18846257]

[86]. Fang J, Wang H, Zhou J, Dai W, Zhu Y, Zhou Y, Wang X, Zhou M, Baicalin provides neuroprotection in traumatic brain injury mice model through Akt/Nrf2 pathway, Drug Design, Development and Therapy, Volume 12 (2018) 2497–2508. [PubMed: 30127597]

[87]. Cui C, Wang C, Jin F, Yang M, Kong L, Han W, Jiang P, Calcitriol confers neuroprotective effects in traumatic brain injury by activating Nrf2 signaling through an autophagy-mediated mechanism, Molecular Medicine, 27 (2021).

[88]. Rashno M, Sarkaki A, Farbood Y, Rashno M, Khorsandi L, Naseri MKG, Dianat M, Therapeutic effects of chrysin in a rat model of traumatic brain injury: A behavioral, biochemical, and histological study, Life Sciences, 228 (2019) 285–294. [PubMed: 31063733]

[89]. Cheng T, Wang W, Li Q, Han X, Xing J, Qi C, Lan X, Wan J, Potts A, Guan F, Wang J, Cerebroprotection of flavanol (−)-epicatechin after traumatic brain injury via Nrf2-dependent and -independent pathways, Free Radical Biology and Medicine, 92 (2016) 15–28. [PubMed: 26724590]

[90]. Armstead WM, Mirro R, Thelin OP, Shibata M, Zuckerman SL, Shanklin DR, Busija DW, Leffler CW, Polyethylene glycol superoxide dismutase and catalase attenuate increased blood-brain barrier permeability after ischemia in piglets, Stroke, 23 (1992) 755–762. [PubMed: 1579974]

[91]. Thorogood MC, Armstead WM, Influence of polyethylene glycol superoxide dismutase/catalase on altered opioid-induced pial artery dilation after brain injury, Anesthesiology, 84 (1996) 614–625. [PubMed: 8659790]

[92]. Hamm RJ, Temple MD, Pike BR, Ellis EF, The effect of postinjury administration of polyethylene glycol-conjugated superoxide dismutase (pegorgotein, Dismutec) or lidocaine on behavioral function following fluid-percussion brain injury in rats, J Neurotrauma, 13 (1996) 325–332. [PubMed: 8835800]

[93]. Lamtai M, Chaibat J, Ouakki S, Zghari O, Mesfioui A, El Hessni A, Rifi EH, Marmouzi I, Essamri A, Ouichou A, Effect of Chronic Administration of Nickel on Affective and Cognitive Behavior in Male and Female Rats: Possible Implication of Oxidative Stress Pathway, Brain Sci, 8 (2018).

[94]. Gaignard P, Savouroux S, Liere P, Pianos A, Thérond P, Schumacher M, Slama A, Guennoun R, Effect of Sex Differences on Brain Mitochondrial Function and Its Suppression by Ovariectomy and in Aged Mice, Endocrinology, 156 (2015) 2893–2904. [PubMed: 26039154]

[95]. Das M, Dixit R, Seth PK, Mukhtar H, Glutathione-S-transferase activity in the brain: species, sex, regional, and age differences, J Neurochem, 36 (1981) 1439–1442. [PubMed: 7264640]

[96]. Chou MY, Chen YJ, Lin LH, Nakao Y, Lim AL, Wang MF, Yong SM, Protective Effects of Hydrolyzed Chicken Extract (Probeptigen(R)/Cmi-168) on Memory Retention and Brain Oxidative Stress in Senescence-Accelerated Mice, Nutrients, 11 (2019).

[97]. Lazarus RC, Buonora JE, Jacobowitz DM, Mueller GP, Protein carbonylation after traumatic brain injury: cell specificity, regional susceptibility, and gender differences, Free Radical Biology and Medicine, 78 (2015) 89–100. [PubMed: 25462645]

[98]. Free KE, Greene AM, Bondi CO, Lajud N, de la Tremblaye PB, Kline AE, Comparable impediment of cognitive function in female and male rats subsequent to daily administration of haloperidol after traumatic brain injury, Exp Neurol, 296 (2017) 62–68. [PubMed: 28698031]

[99]. Taylor AN, Tio DL, Paydar A, Sutton RL, Sex Differences in Thermal, Stress, and Inflammatory Responses to Minocycline Administration in Rats with Traumatic Brain Injury, Journal of Neurotrauma, 35 (2018) 630–638. [PubMed: 29179648]

[100]. Clevenger AC, Kim H, Salcedo E, Yonchek JC, Rodgers KM, Orfila JE, Dietz RM, Quillinan N, Traystman RJ, Herson PS, Endogenous Sex Steroids Dampen Neuroinflammation and Improve Outcome of Traumatic Brain Injury in Mice, Journal of Molecular Neuroscience, 64 (2018) 410–420. [PubMed: 29450697]

[101]. Shuvaev VV, Han J, Tliba S, Arguiri E, Christofidou-Solomidou M, Ramirez SH, Dykstra H, Persidsky Y, Atochin DN, Huang PL, Muzykantov VR, Anti-inflammatory effect of targeted delivery of SOD to endothelium: mechanism, synergism with NO donors and protective effects in vitro and in vivo, PLoS One, 8 (2013) e77002. [PubMed: 24146950]

[102]. Han J, Shuvaev VV, Muzykantov VR, Catalase and superoxide dismutase conjugated with platelet-endothelial cell adhesion molecule antibody distinctly alleviate abnormal endothelial permeability caused by exogenous reactive oxygen species and vascular endothelial growth factor, J Pharmacol Exp Ther, 338 (2011) 82–91. [PubMed: 21474567]

[103]. Shuvaev VV, Christofidou-Solomidou M, Bhora F, Laude K, Cai H, Dikalov S, Arguiri E, Solomides CC, Albelda SM, Harrison DG, Muzykantov VR, Targeted detoxification of selected reactive oxygen species in the vascular endothelium, J Pharmacol Exp Ther, 331 (2009) 404–411. [PubMed: 19692634]

[104]. Gutteridge JM, Lipid peroxidation and antioxidants as biomarkers of tissue damage, Clinical Chemistry, 41 (1995) 1819–1828. [PubMed: 7497639]

[105]. Xu J, Wang H, Ding K, Zhang L, Wang C, Li T, Wei W, Lu X, Luteolin provides neuroprotection in models of traumatic brain injury via the Nrf2–ARE pathway, Free Radical Biology and Medicine, 71 (2014) 186–195. [PubMed: 24642087]

[106]. Ansari MA, Roberts KN, Scheff SW, Oxidative stress and modification of synaptic proteins in hippocampus after traumatic brain injury, Free Radical Biology and Medicine, 45 (2008) 443–452. [PubMed: 18501200]

[107]. Glantz SB, Cianci CD, Iyer R, Pradhan D, Wang KK, Morrow JS, Sequential degradation of alphaII and betaII spectrin by calpain in glutamate or maitotoxin-stimulated cells, Biochemistry-Us, 46 (2007) 502–513.

[108]. Yan XX, Jeromin A, Jeromin A, Spectrin Breakdown Products (SBDPs) as Potential Biomarkers for Neurodegenerative Diseases, Curr Transl Geriatr Exp Gerontol Rep, 1 (2012) 85–93. [PubMed: 23710421]

[109]. Kobeissy FH, Liu MC, Yang Z, Zhang Z, Zheng W, Glushakova O, Mondello S, Anagli J, Hayes RL, Wang KKW, Degradation of βII-Spectrin Protein by Calpain-2 and Caspase-3 Under

Neurotoxic and Traumatic Brain Injury Conditions, Molecular Neurobiology, 52 (2014) 696–709. [PubMed: 25270371]

[110]. Beer R, Franz G, Srinivasan A, Hayes RL, Pike BR, Newcomb JK, Zhao X, Schmutzhard E, Poewe W, Kampfl A, Temporal profile and cell subtype distribution of activated caspase-3 following experimental traumatic brain injury, J Neurochem, 75 (2000) 1264–1273. [PubMed: 10936210]

[111]. Pike BR, Zhao X, Newcomb JK, Posmantur RM, Wang KK, Hayes RL, Regional calpain and caspase-3 proteolysis of alpha-spectrin after traumatic brain injury, Neuroreport, 9 (1998) 2437–2442. [PubMed: 9721910]

[112]. Pike BR, Flint J, Dutta S, Johnson E, Wang KK, Hayes RL, Accumulation of non-erythroid alpha II-spectrin and calpain-cleaved alpha II-spectrin breakdown products in cerebrospinal fluid after traumatic brain injury in rats, J Neurochem, 78 (2001) 1297–1306. [PubMed: 11579138]

[113]. Shuvaev VV, Muro S, Arguiri E, Khoshnejad M, Tliba S, Christofidou-Solomidou M, Muzykantov VR, Size and targeting to PECAM vs ICAM control endothelial delivery, internalization and protective effect of multimolecular SOD conjugates, J Control Release, 234 (2016) 115–123. [PubMed: 27210108]

[114]. Shuvaev VV, Tliba S, Pick J, Arguiri E, Christofidou-Solomidou M, Albelda SM, Muzykantov VR, Modulation of endothelial targeting by size of antibody-antioxidant enzyme conjugates, J Control Release, 149 (2011) 236–241. [PubMed: 21044652]

[115]. Muro S, Cui X, Gajewski C, Murciano JC, Muzykantov VR, Koval M, Slow intracellular trafficking of catalase nanoparticles targeted to ICAM-1 protects endothelial cells from oxidative stress, Am J Physiol Cell Physiol, 285 (2003) C1339–1347. [PubMed: 12878488]

[116]. Chacko AM, Han J, Greineder CF, Zern BJ, Mikitsh JL, Nayak M, Menon D, Johnston IH, Poncz M, Eckmann DM, Davies PF, Muzykantov VR, Collaborative Enhancement of Endothelial Targeting of Nanocarriers by Modulating Platelet-Endothelial Cell Adhesion Molecule-1/CD31 Epitope Engagement, Acs Nano, 9 (2015) 6785–6793. [PubMed: 26153796]

[117]. Zhang W, Mehta A, Tong Z, Esser L, Voelcker NH, Development of Polymeric Nanoparticles for Blood-Brain Barrier Transfer-Strategies and Challenges, Adv Sci (Weinh), 8 (2021) 2003937. [PubMed: 34026447]

[118]. Shuvaev VV, Kiseleva RY, Arguiri E, Villa CH, Muro S, Christofidou-Solomidou M, Stan RV, Muzykantov VR, Targeting superoxide dismutase to endothelial caveolae profoundly alleviates inflammation caused by endotoxin, J Control Release, 272 (2018) 1–8. [PubMed: 29292038]

[119]. Ashok A, Andrabi SS, Mansoor S, Kuang Y, Kwon BK, Labhasetwar V, Antioxidant Therapy in Oxidative Stress-Induced Neurodegenerative Diseases: Role of Nanoparticle-Based Drug Delivery Systems in Clinical Translation, Antioxidants (Basel), 11 (2022).

[120]. Han J, Shuvaev VV, Muzykantov VR, Targeted interception of signaling reactive oxygen species in the vascular endothelium, Ther Deliv, 3 (2012) 263–276. [PubMed: 22834201]

[121]. Hood E, Simone E, Wattamwar P, Dziubla T, Muzykantov V, Nanocarriers for vascular delivery of antioxidants, Nanomedicine (London, England), 6 (2011) 1257–1272. [PubMed: 21929460]

[122]. Shuvaev VV, Muzykantov VR, Targeted modulation of reactive oxygen species in the vascular endothelium, J Control Release, 153 (2011) 56–63. [PubMed: 21457736]

Highlights

- Pro-NP™ is a nanoparticle comprising antioxidant enzymes with burst and sustained release
- Pro-NP™ showed higher accumulation in the brain lesion when injected immediately after injury
- Pro-NP™ scavenged ROS following injury in a controlled cortical impact mouse model of TBI
- Pro-NP™ reduced carbonyl stress in the subacute, but not chronic, phase of injury
- Pro-NP™ delayed the spread of necrosis into the contralateral hemisphere in males but not females

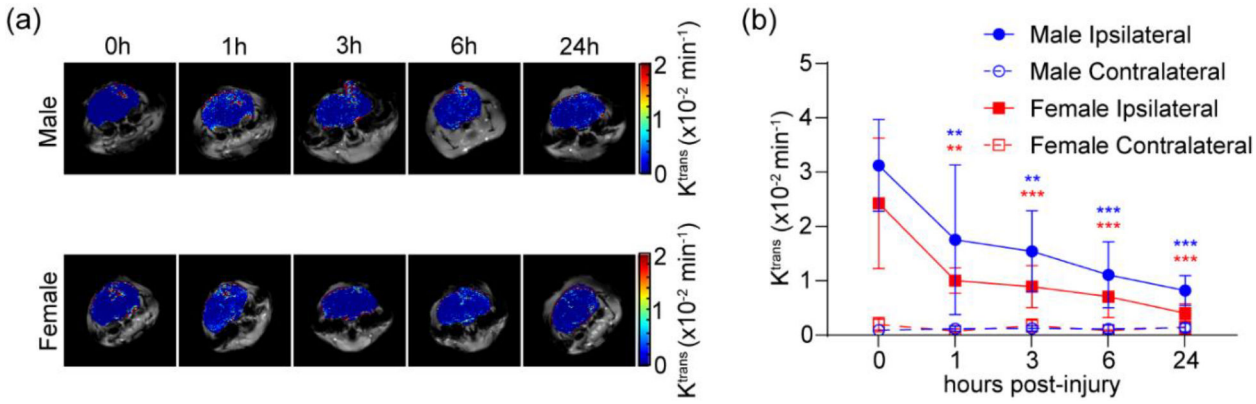

Figure 1.

Identification of treatment window of Gd-Pro-NP™. K^{trans} of Gd-Pro-NP™ in male and female CCI mice in the lesion and contralateral hemisphere at various time points post-injury. (a) Representative K^{trans} mapping of Gd-Pro-NP™. (b) Quantification of K^{trans} mapping in the lesion. Gd-Pro-NP™ accumulated in the lesion the most when administered immediately following the injury (0 h post-injury). Data are shown as mean ± SD with n = 6 for male mice and n = 3 for female mice. * indicates a statistical difference compared to 0 h post-injury group, with two and three symbols indicating $p < 0.01$ and $p < 0.001$, respectively, as determined by one-way ANOVA and Dunnett's post hoc test.

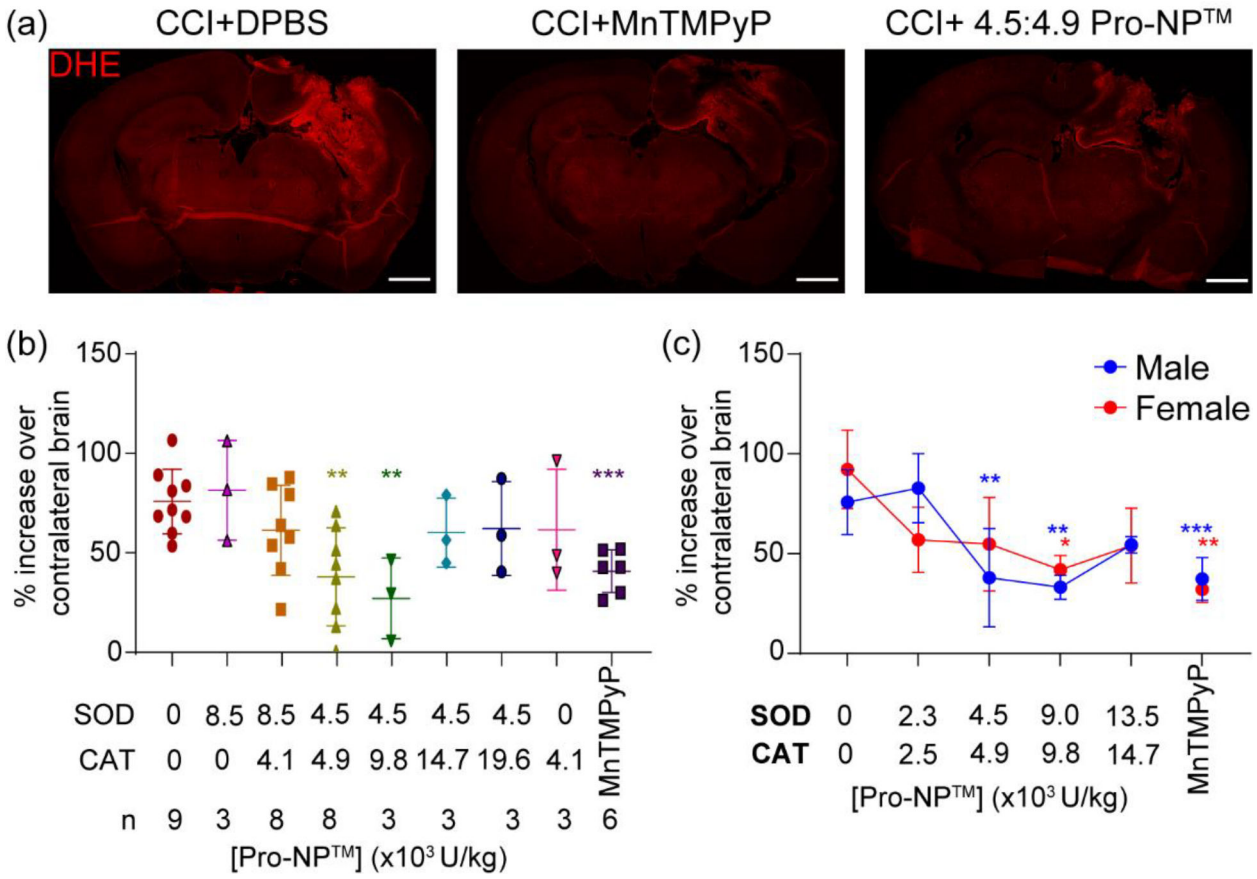

Figure 2.

Identifying the optimum SOD1:CAT activities of Pro-NP™. *In vivo* DHE staining of the brains at 4 h post-injury was utilized to measure the ROS level in the acute phase of injury. Various concentrations and ratios of SOD1:CAT-Pro-NP™ were administered to find the optimum concentration in reducing ROS. (a) Representative confocal microscopy images of control, MnTMPyP, and 4.5:4.9 SOD1:CAT-Pro-NP™ following CCI in male mice. Scale bar is 1 mm. (b&c) Quantification of DHE fluorescence mean intensity at the perilesional normalized to the contralateral hemisphere with various SOD1:CAT-Pro-NP™ ratios in male CCI mice (b), and various concentrations of 1:1 SOD1:CAT-Pro-NP™ in male and female CCI mice (c). Data are shown as mean ± SD with n = 3 for female mice, and n = 3–9 for male mice. * indicates a statistical difference compared to the 0 mg/kg Pro-NP™ group, with one, two, and three symbols indicating $p < 0.05$, $p < 0.01$, and $p < 0.001$, respectively, as determined by one-way ANOVA and Dunnett's post hoc test.

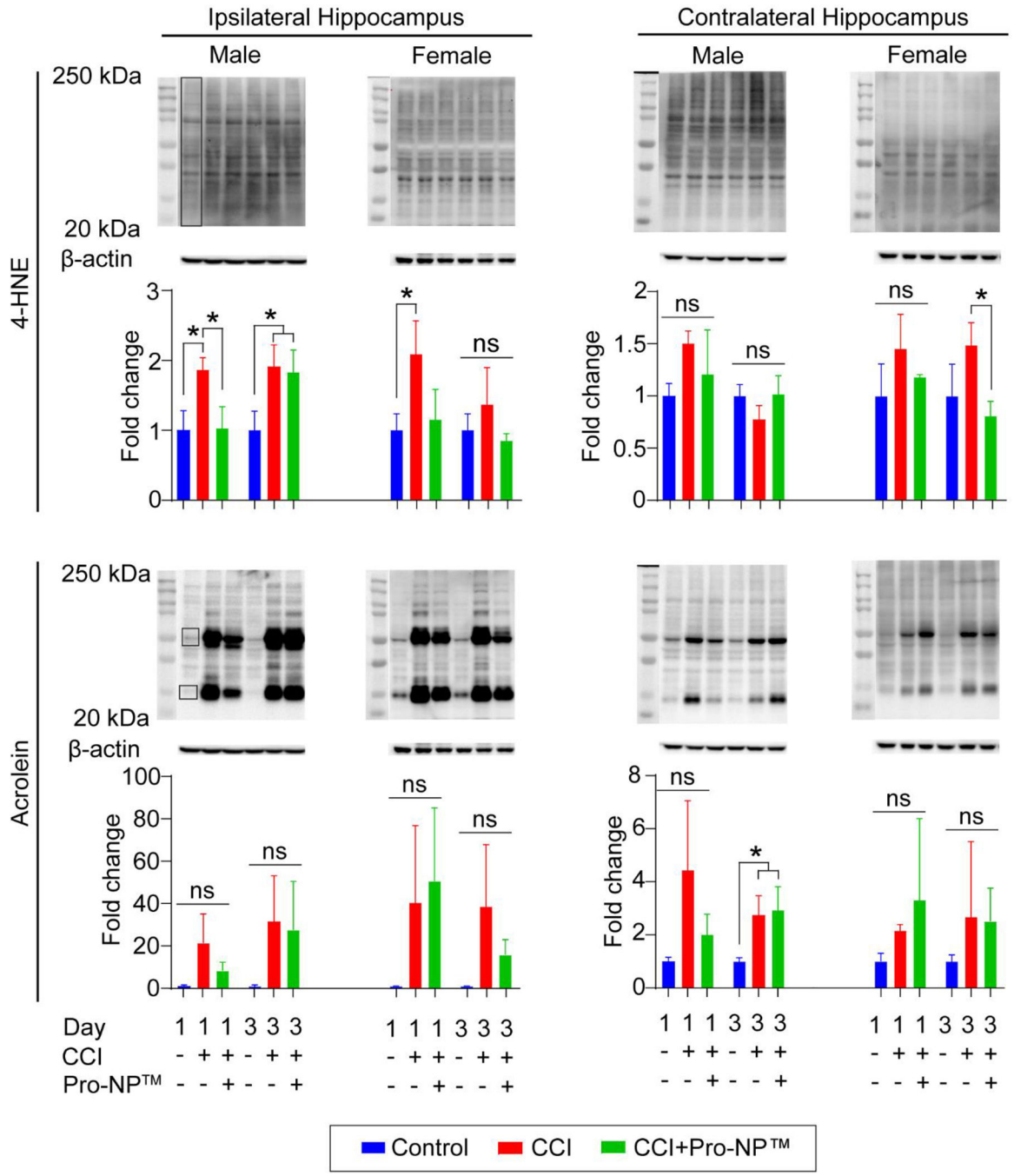

Figure 3.

Analysis of carbonyl stress in the hippocampus. Western blot of 4-HNE and acrolein in the ipsi- and contralateral hippocampus for male and female mice at 1 and 3 d post-injury. The boxed area represents the ROI for quantification of 4-HNE and acrolein in the ipsilateral and contralateral hippocampus normalized to control mice. Data are shown as mean ± SD with n = 3 for each treatment group. ns indicates an insignificant different between treatment group. * indicates a significant different with $p < 0.05$, as determined by one-way ANOVA and Tukey's post hoc test.

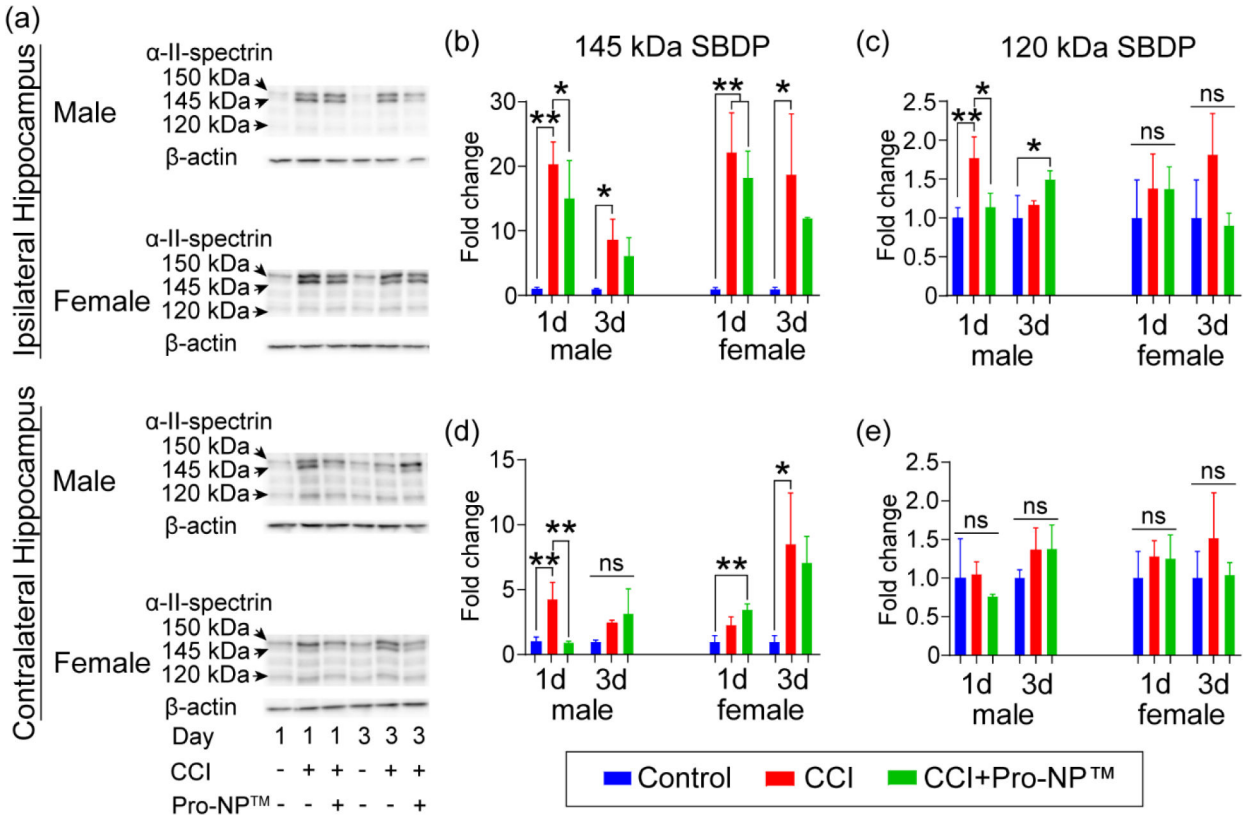

Figure 4.

Analysis of α-II-spectrin breakdown products (SBDPs) in the hippocampus. a) Representative Western blot of α-II-spectrin breakdown products (SBDPs) ipsi- (b,c) and contralateral (d,e) hippocampus for male and female mice at 1 and 3 d post-injury. Quantification of 145 kDa SBDP (proportional to necrosis) (b,d) and 120 kDa SBDP (proportional to apoptosis) (c,e) normalized to control mice, respectively. Data are shown as mean ± SD with n = 3 for each treatment group. ns indicates an insignificant different between treatment group. * and ** indicate a significant different with $p < 0.05$ and $p < 0.01$, respectively, as determined by one-way ANOVA and Tukey's post hoc test.

Table 1.

Properties of Pro-NP™s used for K^{trans} imaging and antioxidant therapy.

Particle	Size (nm)	PDI	Resuspended size (nm)	Resuspended PDI	Zeta potential (mV)	Initial burst enzyme activity (U/mg Pro-NP™)	Sustained release enzyme activity (U/mg Pro-NP™)	Gd concentration (mmol/mg Pro-NP™)
Gd-Pro-NP™	214	0.036	292	0.131	−10.3	~	~	7.56×10^{-6}
SOD1-Pro-NP™	203	0.12	274	0.132	−15.3	658	43	~
CAT-Pro-NP™	218	0.103	284	0.117	−25.7	298	37	~